Indian Journal of Natural Products and Resources
Vol. 12(2), June 2021, pp. 173-180

Bestatin is a non-competitive inhibitor of porcine M1 family glutamyl aminopeptidase: Insights for selective inhibitor design

Mario E. Valdés-Tresanco[1,2], Yarini Arrebola Sánchez[1], Laura Rivera Méndez[1], Fabiola Almeida[1], Belinda Sánchez[3], Jean-Louis Charli[4] and Isel Pascual Alonso[1]*

[1]Center for Protein Studies, Faculty of Biology, University of Havana, Havana, Cuba

[2]Department of Biological Sciences, University of Calgary, Calgary, Canada

[3]Centro de Inmunología Molecular, Habana, Cuba

[4]Instituto de Biotecnología, Universidad Nacional Autónoma de México (UNAM), Cuernavaca, Morelos, México

Received 18 July 2020; Revised 01 March 2021

Glutamyl aminopeptidase (APA) is an M1 family membrane-bound ectoenzyme that is a target for the development of antihypertensive and anticancer agents. Bestatin is a natural product described as a classical inhibitor of metallo-aminopeptidases. Although the IC_{50} value of bestatin vs human APA has been reported, the mechanism of inhibition is unknown. In the present contribution, we demonstrated that bestatin is a non-competitive ($\alpha>1$) inhibitor of porcine APA (pAPA), with a K_i value of 31.59 μM ($\alpha=3.7$). A model of the bestatin-pAPA complex predicted that bestatin binds to pAPA similarly to porcine aminopeptidase N (pAPN). The interaction involved catalytic and chelating residues conserved in the M1 family. Additionally, a salt bridge with R877 and a hydrogen bond interaction with T346, both key residues for APA specificity for N-terminal acidic residues were identified. These residues and E213, which forms a hydrogen bond interaction with bestatin, are not conserved in human and porcine APN. The extension of the *in silico* analysis to amastatin and bestatin analogs probestin, and phebestin, which are APA inhibitors, indicated that they may interact with the same residues. The results indicate that bestatin analogues currently reported to inhibit APN are dual inhibitors of APA and APN and that some APA residues could be targeted to improve inhibitor selectivity.

Keywords: Amastatin, Bestatin, Glutamyl aminopeptidase, Non-competitive inhibitors, Phebestin, Probestin.

IPC code; Int. cl. (2015.01)- A61K 36/00

Introduction

Aminopeptidase A (APA, EC 3.4.11.7) is a M1 family (Clan MA(E)) mammalian type II integral membrane zinc-containing metallopeptidase that hydrolyzes peptides with a N-terminal acidic residue. In the enzymes of this clan, the Zn^{2+} atom is linked to the protein through two His residues, which are part of the HEXXH consensus sequence. In addition to the His residues, the catalytic Zn^{2+} is coordinated by a water molecule and a third residue, Glu, located at least 14 residues after the carboxyl terminus of the HEXXH sequence[1,2]. APA monomer molecular weight is 109 kDa for the human isoform and 108 kDa for the porcine isoform[1]. APA's S1 pocket is structured to accommodate acid residue side chains, hydrolyzing N-terminal aspartic and glutamic residues[3]. In addition to the catalytic Zn^{2+}, APA binds Ca^{2+}, an association that increases its enzymatic activity. This enzyme is widely distributed in mammalian tissues and constitutively expressed by the nervous system and by proximal tubule cells[4,5]. APA performs fundamental functions in a wide range of physiological processes. It participates in the metabolism of angiotensin II and the formation of angiotensin III, one of the main effector peptides of the renin-angiotensin-aldosterone system in the central nervous system, making it an important regulator of blood pressure[2,3,6,7]. In addition, it is involved in pathophysiological processes such as the development of Alzheimer's disease, glomerulosclerosis, and the progression of cancer. It is associated with the development of renal neoplasms, malignant trophoblasts, renal choriocarcinoma, and colorectal cancer[8-12]. APA is thus a current target for the development of antihypertensive[7] and anticancer agents[13].

Bestatin is a natural product, a classical inhibitor of metallo-aminopeptidases from the M1 and M17 families, with antitumoral and antiplasmodial effects[2,14-16]. Bestatin is a non-competitive ($\alpha>1$) inhibitor of human and

*Correspondent author
Email: isel@fbio.uh.cu
Supplementary figures are available online only

porcine neutral aminopeptidase (APN)[15]. This enzyme is the most extensively studied member of the M1 family of aminopeptidases and catalyzes the cleavage of neutral and basic amino acids from the N-terminus of protein or peptide substrates[2]. APN is a current target for the development of antihypertensive and anticancer agents[14]. Although structural and kinetic studies describe the interaction of bestatin with human APA[3], there is no mechanistic study that establishes the type of inhibition of mammalian APA by bestatin. Since porcine kidney APA (pAPA) has biochemical and functional properties similar to those of its human orthologue[17], the authors studied the type of inhibition of pAPA by bestatin using a kinetic approach and predicted structural determinants of their interaction. The authors identified for the first time that the inhibition is non-competitive ($\alpha>1$). According to modelling data, various non-conserved residues as targets to improve the selectivity of bestatin analogues for APA *vs* other members of the M1 family are proposed.

Materials and Methods

Materials and reagents

Microsomes containing pAPA were prepared as previously described[18]. The chromogenic synthetic substrate of pAPA, L-Glutamyl-p-nitroanilide (L-Glu-pNA), and bestatin were purchased from Bachem. The remaining reagents were of analytical grade. A Genesys 10 UV light passage cuvette spectrophotometer, Thermo Electron Corporation, was used for Enzyme Activity (EA) assays of pAPA.

Porcine APA enzymatic activity

Enzymatic activity of microsomal pAPA (0.1 mg/mL) was determined using the specific chromogenic synthetic substrate L-Glu-p-NA in buffer Tris-HCl 50 mM pH 8.0, 1 mM of $CaCl_2$, 0.1% of Triton X100 (Buffer A), to complete a final assay volume of 1 mL, as previously described[17]. The use of the specific acidic substrate, and the presence of calcium in the system, allowed us to specifically determine the activity of APA and the effect of bestatin, on this enzyme present in the complex mixture of the microsomal preparation.

In vitro inhibition of pAPA activity by bestatin: pre-incubation time and dose-response

Bestatin was prepared as a stock solution of 10 mM in DMSO and diluted to obtain the desired range of concentrations in Buffer A. The preliminary effect of bestatin on pAPA was tested at 1, 10, 100 µM to identify the range of inhibition. Pre-incubation time for equilibrium was determined by enzyme incubation with 20 µM of bestatin for 0, 1, 5, 10, 30 or 60 min, before the addition of L-Glu-p-NA. The dose-response effect of bestatin was determined by quantifying the decrease of activity in aliquots pre-incubated with the inhibitor (1 to 500 µM) for 30 minutes at 37 °C (n=4)[19]. The IC_{50} value (half maximal inhibitory concentration) was determined by nonlinear regression of all the data of residual activity from the dose-response curve using the IC_{50} equation included in the software GraphPadPrism 9.0.

Kinetic mechanism of inhibition of pAPA by bestatin

Since the IC_{50} value of bestatin vs pAPA was higher than 10^{-7} M, a Michaelis-Menten approach was followed to study the kinetic mechanism of classical reversible inhibition. Enzyme assays were conducted at increasing L-Glu-pNA concentration (0.18-1.75 mM) and 5-100 µM bestatin (n=4). Enzyme and inhibitor were pre-incubated at 37 °C for 30 minutes to attain equilibrium. The data were transformed and fitted to the Lineweaver-Burk (LB) model for diagnosis of the mechanism and to determine the slope and Y-axis intercept ($1/V_{max\ app}$) of the line at each inhibitor concentration. With the primary data of intercepts and slopes, two secondary plots were used, as recommended by Copeland[19]: a) a Dixon plot of $1/V_{max\ app}$ as a function of inhibitor concentration, for determination of the αK_i value (X intercept) and b) a plot of the LB slopes as a function of inhibitor concentration for determination of the K_i value (X intercept). Combining information from these two secondary plots allows the determination of both inhibitor dissociation constants from a single set of experimental data.

Bioinformatic analysis

Structural modelling of pAPA:inhibitor complexes

Since human and porcine APAs have a high degree of sequence identity (~80% overall, ~100% for active site residues), we modelled the complexes between inhibitors and pAPA. Considering that bestatin interacts similarly with the human and porcine enzymes, we used Modeller to obtain the possible complexes by extracting and satisfying distance restraints automatically[20]. The structure of human APA (PDB ID: 4KXB) in complex with bestatin was used as a template. A similar strategy was used for modelling the pAPA: amastatin complex using the human APA: amastatin structure (PDB ID: 4KX8). The complexes with bestatin derivates phebestin and probestin were obtained by using the structure of human APA (PDB ID: 4KXB) in complex with bestatin as a template; phebestin and probestin were aligned to bestatin bound in the APA active site; then, Modeller was used for generating the complex between these

ligands and pAPA by extracting and satisfying distance restraints automatically[20]. In all the cases, an energy minimization step using the "Minimize Structure" module from Chimera software[21] was performed. Zinc and atoms belonging to the coordinating residues were kept fixed during the minimization process; other parameters were kept as default. Finally, the quality of the homology models was assessed with ERRAT[22] and Verify3D[23] using SAVES6.0 online server (https://saves.mbi.ucla.edu/). Models had a high overall quality factor (>90), which characterizes the amount and quality of the non-bonded interactions between different atom types (Table 1). Poor quality regions were far from the active site, and we concluded they should not affect the modeling of the enzyme: substrate interaction (Fig. S1). On the other hand, the compatibility of an atomic model (3D) with its amino acid sequence (1D) was high (>96%) (Table 1).

Generation of the pAPA:L-Glu-pNA complex

A 3D structure of L-Glu-pNA substrate bound to the porcine APA active site was generated by docking. The structure of human APA bound to glutamate was used as template to assure glutamate side chain was properly oriented into APA's S1 site. AutoDock4Zn was used for docking[24] through AMDock program[25]. The grid maps were calculated with AutoGrid. The grid dimensions were 18 Å × 18 Å × 18 Å with grid spacing 0.375 Å and grid centre defined at the centre of mass of Zn atom. L-Glu-pNA was kept flexible in the grid box while the protein was kept rigid. Other docking parameters were kept as default.

Generation of the terciary complex: docking of bestatin to the pAPA:L-Glu-pNA enzyme:substrate complex

To obtain the predicted structure of the terciary complex, the enzyme: substrate structure was used as a receptor in bestatin docking. Bidimensional structures (2D) of bestatin in Structure Data File format were used to generate the 3D structure by using Avogadro[26]. Docking was performed as described before, keeping bestatin flexible while the enzyme: substrate complex was kept rigid. The grid maps were calculated with AutoGrid. The grid dimensions were 21 Å × 21 Å × 18 Å with grid spacing 0.375 Å and grid centre defined at the centre of mass of L-Glu-pNA substrate.

Sequence analysis

The multiple sequence alignment of porcine APA (AMPE_PIG), human APA (AMPE_HUMAN), human APN (AMPN_HUMAN), porcine APN (AMPN_PIG), and human endoplasmic reticulum aminopeptidase 1 (ERAP1_HUMAN) was performed using the Clustal W software[27]. The multiple alignments were manually parsed by analyzing the gaps, conserved amino acid regions and the secondary structure information using Seaview software[28].

Table 1 — Quality assessment of APA: inhibitor models with ERRAT and Verify3D algorithms

Model	ERRAT *	Verify3D **
APA:bestatin	94.9	96.02
APA:amastatin	90.1	96.11
APA:phebestin	94.7	96.13
APA:probestin	95.0	96.10

* Overall quality factor

** % of residues that have an averaged 3D-1D score ≥ recommended score (0.2)

Results

Kinetic characterization of microsomal pAPA inhibition by bestatin

At 0.25 mM substrate concentration pAPA was dose-dependently inhibited by 1-100 µMbestatin (Fig. S2a); 30 minutes pre-incubation with 20 µM bestatin was sufficient to attain equilibrium (Fig. S2b). Dose-response studies were performed using 30 minutes pre-incubation. Bestatin effect on APA

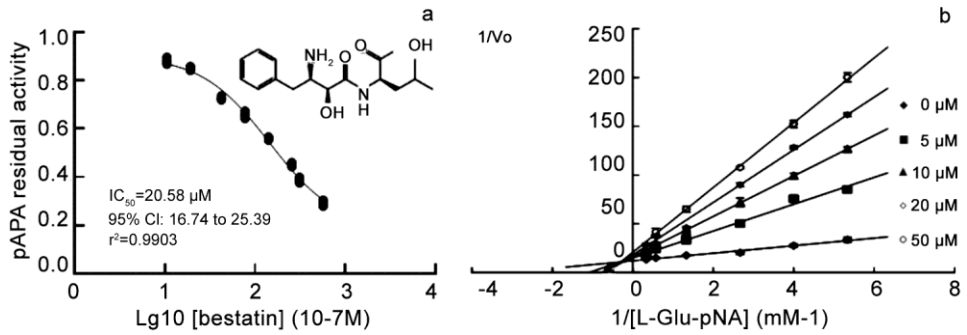

Fig. 1 — Biochemical analysis of the mode of interaction of bestatin with pAPA; a): Dose-response curve (data are individual values (n=4)); the 2D structure of bestatin is shown, b): Lineweaver-Burk plot for diagnosis of the modality of pAPA inhibition by bestatin (Data are mean±SD, n=4)

activity was dose-dependent (Fig. 1a). IC_{50} was 20.58 µM (95% CI: 16.74 to 25.39 µM, r^2=0.9903), suggesting bestatin acts as a classical inhibitor. The kinetic mechanism of inhibition was studied using the Lineweaver-Burk (LB) approach[19]. The pattern of straight lines in the double-reciprocal plot is the signature for a typical non-competitive (α>1) inhibition (Fig. 1b). This means that bestatin displays a binding affinity for both the free enzyme and the enzyme-substrate binary complex. This mode of inhibition is also referred to in the literature as "mixed" inhibition since it manifests at increasing inhibitor concentration as a combination of decreased V_{max} (indicative of a reduction in the catalytic efficiency) and increased K_M (indicative of a reduction in the substrate affinity). Two secondary plots, LB slopes vs inhibitor concentration (Fig. S3a) and $1/V_{max}$ vs inhibitor concentration (Fig. S3b) led to a K_i value of 31.59 µM with α=3.7 for the pAPA-bestatin interaction. This α value indicates that bestatin binds free pAPA with almost 4-fold higher affinity than the enzyme: substrate complex.

Bioinformatic studies of the porcine APA interaction with bestatin and other natural inhibitors

To figure out how bestatin inhibits pAPA, we analyzed the binding mode of the inhibitor to the porcine enzyme obtained by homology modelling. We addressed inhibitor interactions with residues enrolled in catalysis,substrate-binding and other putative subsites. The modelling of the pAPA: bestatin complex (Fig. 2a) showed that the inhibitor accommodated in a pose that includes interactions with residues H^{383}, E^{384}, H^{387} associated with zinc chelation, and E^{406} and Y^{469} implicated in catalysis. These interactions support the non-competitive type of inhibition identified by the kinetic approach and the effect on V_{max} at increasing inhibitor concentration.

The S1 pocket of human APA is well suited to accommodate the side chains of acidic residues. Our analysis showed a salt bridge interaction between the C-terminal carboxylate of bestatin and the guanidinium moiety of pAPA R^{877}(R^{887} in human APA, R^{878} in mouse APA), a key residue in the interaction of the substrate with the APA active site. This interaction between bestatin and R^{887}supports the competitive component of the identified non-competitive inhibition (α>1). Additionally, we detected a hydrogen bond interaction with T^{346}, which plays a key role in the substrate specificity of APA for N-terminal acidic amino acids. Bestatin also forms a hydrogen bond interaction with pAPA E^{213} that is not conserved in human and porcine APN.

To better understand the non-competitive inhibition profile, it was critical to address inhibitor interactions with residues enrolled in the substrate-binding pocket and other putative subsites. Therefore, we docked the substrate in the active site of pAPA and subsequently generated the terciary complex APA: substrate: inhibitor. Although a couple of salt bridge interactions with R^{877} and R^{881}were spotted in the terciary complex, the number of interactions of bestatin with the enzyme: substrate complex was lower than with the free enzyme (Fig. S4). This is expected for a non-competitive (α>1) inhibition profile in which bestatin binds free pAPA with almost 4-fold higher affinity than the enzyme: substrate complex.

Taking into account these findings, the authors extended the *in silico* structural analysis to other natural M1 family inhibitors, such as the natural bestatin analogues probestin (IC_{50} vs pAPA 19.0 µM)[29] and phebestin (IC_{50} vs pAPA 20 µM)[30], and amastatin (K_i vs hAPA 74.0 nM)[3]. There is no information regarding the structural basis of porcine APA inhibition by these molecules. Phebestin (Fig. 2b) and probestin (Fig. 2c) accommodated in a pose similar to that of bestatin, with similar interactions. Phebestin made an additional cation-pi interaction with the lateral group of R^{881}. Amastatin fit into the S3'subsite of pAPA, forming a salt bridge with R^{376}. However, the binding of amastatin (Fig. 2d) was slightly different to that of bestatin, probestin and phebestin, with a higher number of hydrogen bonds and an interaction with N^{878}.

Discussion

Bestatin is a very well known inhibitor of M1 and M17 metallo aminopeptidases[2], but knowledge about its effect on APA was limited to some biochemical and structural data for its interaction with human APA[3]. There was no mechanistic study that establishes the type of inhibition of mammalian APA by bestatin. In the present contribution, we identified by kinetic assays the mechanism of inhibition of bestatin vs porcine APA. Dose-response studies revealed IC_{50} values in the micromolar range, suggesting bestatin acts as a classical inhibitor. This IC_{50} value is in the same order as that of other bestatin derived inhibitors of the M1 family, although for most of them there are no data regarding APA inhibition[14,31,32]. The Lineweaver-Burk approach applied to the kinetic data strongly supports a non-competitive inhibition (α > 1). This mechanism was previously shown for bestatin vs porcine kidney APN

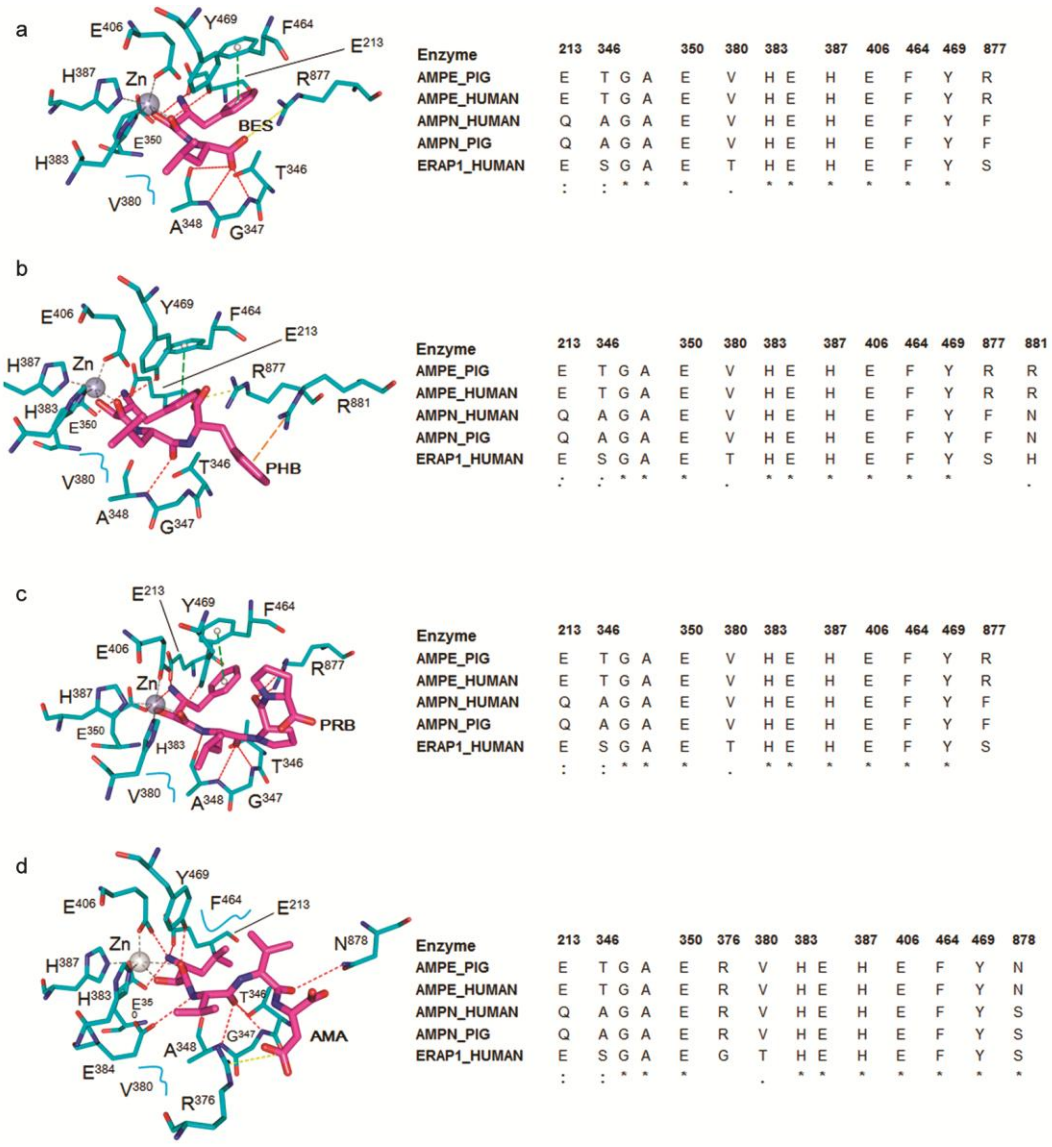

Fig. 2 — Predicted binding mode of pAPA complexes with natural inhibitors and alignment of contact residues among several M1 aminopeptidases. Ligands have been represented as sticks (C: magenta, N: blue, O: red) while APA active site residues as lines (C: cyan, N: blue, O: red). The Zn atom is represented as a grey sphere. Hydrogen bond interactions are represented as red dashed lines, salt bridges as yellow dashed lines, pi-pi stacking as green dashed lines, cation-pi interactions as orange dashed lines, and Zn coordination as grey dashed lines. For clarity, residues interacting only via van der Waals bonds are represented as cyan curved lines. Uniprot codes: porcine APA (AMPE_PIG); human APA (AMPE_HUMAN), human APN (AMPN_HUMAN), porcine APN (AMPN_PIG), human endoplasmic reticulum aminopeptidase (ERAP1_HUMAN). (a) pAPA: bestatin (BES) complex; (b) pAPA:phebestin (PHB) complex; (c) pAPA: probestin (PRB) complex; (d) pAPA: amastatin (AMA) complex.

and human placental APN[16], as well as for bestatin vs *Escherichia coli* APN (PepN)[32]. The K_i value of 31.59 µM determined for the pAPA-bestatin interaction is lower than previously reported for the human APA (K_i: 75 µM) using a similar substrate, but a different kinetic approach[3]. In the latter case, the K_i value for the human enzyme was determined from the IC_{50} value assuming a competitive mode of inhibition[3]. In this work, the crystallographic structure of human APA bound to bestatin was experimentally determined and the authors found that bestatin targets the active site and partially binds the S1 pocket. Since the S1 pocket is the primary determinant for substrate specificity, the authors assumed a competitive inhibition mechanism (i.e., total blockade of substrate binding), without any kinetic experimental validation. However, our experimental data provide clear evidence of non-competitive inhibition (a>1),

indicating that impairment of substrate binding (increment of K_M) by bestatin only contributes partially to the mechanism.

To understand the non-competitive inhibition profile identified for bestatin vs pAPA, we modelled inhibitor interactions with residues enrolled with different subsites involving substrate binding and catalysis. APN and APA share a common catalytic mechanism despite their modest sequence similarity[3,33]. The modelling of the pAPA: bestatin complex shows that the inhibitor accommodated in a pose similar to that previously predicted for the pAPN: bestatin complex[15], including interactions with chelating (H^{383}, E^{384}, H^{387}) and catalytic residues (E^{406} and Y^{469}). These residues are highly conserved inside the M1 family; chelation of zinc ions through a zinc-binding group is the most common mode of action for inhibitors targeting metallo aminopeptidases[14,31,34]. Thus, these data support the non-competitive type of inhibition identified by the kinetic approach.

The S1 pocket accommodating the P1 side chain of ligands differs markedly between APN and APA, consistent with their different substrate specificities. The S1 pocket of human APA is well suited to accommodate the side chains of acidic residues; i.e., the P1 carboxylate side chain forms a strong salt bridge with R^{887} and a hydrogen bond with T^{356} in human APA, and similarly for R^{878} in mouse APA. These energetically favourable interactions are consistent with the high activity that mammalian APA exerts on substrates with glutamate at the P1 site[3,35]. In line with this, our analysis showed interactions of bestatin withpAPA $R^{877}$and T^{346}. This last residue plays a key role in the substrate specificity of APA for N-terminal acidic amino acids by ensuring the optimal positioning of the substrate during catalysis[36]. The sequence analysis of aminopeptidases belonging to the M1 family (Fig. 2a) suggests that targeting the R^{877} and T^{346} residues should improve the selectivity and potency of APA inhibitors regarding other M1 family members, as demonstrated for EC33 [(S)-3-amino-4-mercapto-butyl sulfonic acid] [37] and for NI929 ([3S,4S]-3-amino-4-mercapto-6-phenyl-hexane-1-sulfonic acid)[38]. Additionally, bestatin forms a hydrogen bond interaction with E^{213}, a residue that is not conserved in human and porcine APN, which suggests another clue for the design of selective inhibitors of APA *vs* APN.

Based on the findings with bestatin, we extended the *in silico* structural analysis to other natural metallo aminopeptidases inhibitors. In general, probestin and phebestin showed similar interactions to that of bestatin. In addition, phebestin interacted with the lateral group of R^{881}, a residue not conserved in human and porcine APN and another member of the M1 family, human endoplasmic reticulum aminopeptidase 1. Amastatin fits into the S3'subsite of pAPA, as previously shown for its experimentally determined binding to hAPA[3], with a higher number of hydrogen bonds and an interaction with N^{878}, a residue not conserved in the M1 family. The high number of interactions of amastatin with pAPA is in accordance with a K_i value for hAPA at least three orders of magnitude lower than the K_i value for bestatin-pAPA. These results suggest mechanisms by which bestatin analogues currently reported as inhibitors of APN[31,32,34,39,40] are probably also inhibitors of APA.

There are few examples of non-competitive inhibitors in the literature and clinical use, including against M1 family aminopeptidases like APN and APA[15,17]. Compared to competitive inhibition, non-competitive inhibition is advantageous when physiological context exposes the target enzyme to high substrate concentrations[19]. The mode of inhibition of bestatin and analogues *vs* pAPA is relevant in the context of the development of new antihypertensive agents targeting brain renin-angiotensin system[7], and to treat cancers like renal, cervical, and colorectal carcinomas[13,14,41,42].

Conclusion

Micromolar bestatin inhibits the activity of porcine APA through a non-competitive ($\alpha>1$) mechanism. The K_i value is 2-3 fold lower than previously reported for human APA. The discovery of a non-competitive mechanism is of biomedical relevance for APA inhibitor applications. Additionally, the predictions that bestatin, probestin and phebestin interact with the $R^{877}$and that amastatin interact with N^{878} (both non-conserved residues inside the M1 family), may be useful for the design of bestatin and amastatin analogues selective for APA *vs* other M1 family members.

Conflict of interest

The authors declare no conflict of interest.

Acknowledgements

This work was supported in part by the CIM-UH project: "New inhibitors of aminopeptidases with potential applications in cancer" (2016-2020), grant PN223LH010-010 National Program of Basics and Natural Sciences (PN10, CITMA-Cuba) and by Coordinación de la Investigación Científica, UNAM, Mexico (8862-2019).

References

1 Rawlings N D, Barrett A J, Thomas P D, Huang X, Bateman A, *et al.*, The MEROPS database of proteolytic enzymes, their substrates and inhibitors in 2017 and a comparison with peptidases in the PANTHER database, *Nucleic Acids Res*, 2018, **46**, D624–D632.

2 Drinkwater N, Lee J, Yang W, Malcolm T R and McGowan S, M1 aminopeptidases as drug targets: Broad applications or therapeutic niche?, *FEBS J*, 2017, **284**(10),1473-1488.

3 Yang Y, Liu C, Lin Y L and Li F, Structural insights into central hypertension regulation by human aminopeptidase A, *J Biol Chem*, 2013, **288**(35), 25638–25645.

4 Nanus D M, Bogenrieder T, Papandreou C N, Finstad C L, Lee A , *et al.*, Aminopeptidase A expression and enzymatic activity in primary human renal cancers, *Int J Oncol*, 1998, **13**(2), 261-268.

5 Iturrioz X, Vazeux G, Célérier J, Corvol P and Llorens-Cortès C, Histidine 450 plays a critical role in catalysis and, with Ca2+, contributes to the substrate specificity of aminopeptidase A, *Biochem*, 2000, **39**(11), 3061–3068.

6 Chen Y, Tang H, Seibel W, Papoian R, Oh K, *et al.*, Identification and characterization of novel inhibitors of mammalian aspartyl aminopeptidase, *Mol Pharmacol*, 2014, **86**(2), 231-242.

7 Llorens-Cortes C and Touyz R M, Evolution of a new class of antihypertensive drugs: Targeting the brain renin-angiotensin system, *Hypertension*, 2020, **75**(1), 6-15.

8 Göhring B, Holzhausen H, Meye A, Heynemann H, Rebmann U, *et al.*, Endopeptidase 24.11/CD10 is down-regulated in renal cell, *Int J Mol Med*, 1998, **2**(4), 409-423.

9 Song L and Healy D P, Kidney, Aminopeptidase A and hypertension, Part II. Effects of angiotensin II, *Hypertension*, 1999, **33**(2), 746-752.

10 Tonna S, Dandapani S V, Uscinski A, Appel G B, Schlöndorffa J S, *et al.*, Functional genetic variation in aminopeptidase A (ENPEP): Lack of clear association with focal and segmental glomerulosclerosis (FSGS), *Gene*, 2008, **410**(2), 44-52.

11 Puertas M, Martínez-Martos J M, Cobo M and Lorite P, Sandalio R M, *et al.*, Plasma renin-angiotensin system-regulating aminopeptidase activities are modified in early stage Alzheimer's disease and show gender differences but are not related to apolipoprotein E genotype, *Exp Gerontol*, 2013, **48**(6), 557-564.

12 Blanco L, Sanz B, Perez I, Sánchez C, Cándenas M L, *et al.*, Altered glutamyl-aminopeptidase activity and expression in renal neoplasms, *BMC Cancer*, 2014, **14**(1), 1-9.

13 Chuang H, Jiang J, Yang M, Wang H, Li M, *et al.*, Aminopeptidase A initiates tumorigenesis and enhances tumor cell stemness via TWIST1 upregulation in colorectal cancer, *Oncotarget*, 2017, **8**(13), 21266-21280.

14 Amin A, Adhikari N and Jha T, Design of aminopeptidase N (APN) inhibitors as anticancer agents, *J Med Chem*, 2018, **61**(15), 6468−6490.

15 Pascual I, Valiente P A, García G, Valdés-Tresanco M E, Arrebola Y, *et al.*, Discovery of novel non-competitive inhibitors of mammalian neutral M1 aminopeptidase (APN), *Biochimie*, 2017, **142**, 216-225.

16 Pascual I, Bounaadja L, Sánchez L, Rivera L, Tarnus C, *et al.*, Aqueous extracts of marine invertebrates from Cuba coastline display neutral aminopeptidase inhibitory activities and effects on cancer cells and *Plasmodium falciparum* parasites, *Indian J Nat Prod Resour*, 2017, **8**, 107-119.

17 Arrebola Y, Rivera L, Pedroso A, McGuire R, Valdes-Tresanco M E, *et al.*, Bacitracin is a non-competitive inhibitor of porcine M1 family neutral and glutamyl aminopeptidases, *Nat Prod Res*, 2019, **33**, 1-5

18 Byzia A, Szeffler A, Kalinowski L and Drag M, Activity profiling of aminopeptidases in cell lysates using a fluorogenic substrate library, *Biochimie*, 2016, **122**, 31-37.

19 Copeland R A, *Evaluation of enzyme inhibitors in drug discovery: A guide for medicinal chemists and pharmacologists*, II edn, (John Wiley & Sons, Inc, Hoboken, New Jersey), 2013.

20 Sali A and Blundell T L, Comparative protein modelling by satisfaction of spatial restraints, *J Mol Biol*, 1993, **234**, 779-815.

21 Pettersen E F, Goddard T D, Huang C C, Couch G S, Greenblatt D M, *et al.*, UCSF Chimera--a visualization system for exploratory research and analysis, *J Comput Chem*, 2004, **25**(13), 1605-1612.

22 Colovos C and Yeates T O, Verification of protein structures: Patterns of nonbonded atomic interactions, *Protein Sci*, 1993, **2**(9), 1511-1519.

23 Bowie J U, Lüthy R and Eisenberg D, A method to identify protein sequences that fold into a known three-dimensional structure, *Sci*, 1991, **253**, 164-170.

24 Santos-Martins D, Forli S, Ramos M J and Olson A J, AutoDock4Zn: An improved AutoDock force field for small-molecule docking to zinc metalloproteins, *J Chem Inf Model*, 2014, **54**(8), 2371-2379.

25 Valdés-Tresanco M S, Valdés-Tresanco M E, Valiente P A and Moreno E, AMDock: A versatile graphical tool for assisting molecular docking with Autodock Vina and Autodock4, *Biol Direct*, 2020, **15**(1), 1-12.

26 Hanwell M D, Curtis D E, Lonie D C, Vandermeersch T, Zurek E, *et al.*, Avogadro: An advanced semantic chemical editor, visualization, and analysis platform, *J Cheminform*, 2012, **4**(1), 17.

27 Thompson J D, Higgins D G and Gibson T J, CLUSTAL W: Improving the sensitivity of progressive multiple sequence alignment through sequence weighting, position-specific gap penalties and weight matrix choice, *Nucleic Acids Res*, 1994, **22**, 4673-4680.

28 Galtier N, Gouy M and Gautier C, SEAVIEW and PHYLO_WIN: Two graphic tools for sequence alignment and molecular phylogeny, *Bioinform*, 1996, **12**(6), 543-548.

29 Tieku S and Hooper N M, Inhibition of aminopeptidases N, A and W.A re-evaluation of the actions of bestatin and inhibitors of angiotensin converting enzyme, *Biochem Pharmacol*, 1992, **44**, 1725-1730.

30 Nagai M, Kojima F, Naganawa H, Hamada M, Aoyagi T, *et al.*, A new inhibitor of aminopeptidase N, produced by *Streptomyces sp.* MJ716-m3, *J Antibiot*, 1993, **50**, 82-84.

31 Mucha A, Drag M, Dalton J P and Kafarski P, Metallo-aminopeptidase inhibitors, *Biochimie*, 2010, **92**, 1509-1529.

32 Varela A C, Pérez I, De Armas G, Méndez Y, Izquierdo M, *et al.*, Structure-activity relationship of the inhibition of M1-aminopeptidases from *Escherichia coli* (ePepN) and *Plasmodium falciparum* (PfA-M1) by bestatin-derived peptidomimetics, *Revista Cubana de Ciencias Biológicas*, 2019, **7**, 1-21.

33 Wong A H M, Zhou D and Rini J M, The X-ray crystal structure of human aminopeptidase N reveals a novel dimer and the basis for peptide processing, *J Biol Chem*, 2012, **287**, 36804-36813.

34 Harbut M B, Velmourougane G, Reiss G, Chandramohanadas R and Greenbaum D C, Development of bestatin-based activity-based probes for metalloamino peptidases, *Bioorg Med Chem Lett*, 2008, **18**, 5932–5936.

35 Couvineau P, de Almeida H, Maigret B, Llorens-Cortes C and Iturrioz X, Involvement of arginine 878 together with Ca2+ in mouse aminopeptidase A substrate specificity for N-terminal acidic amino-acid residues, *PLoS One*, 2017,**12**, e0184237.

36 Claperon C, da Banegas-Font I, Iturrioz X, Rozenfeld R, Maigret B, *et al.*, Identification of threonine 348 as a residue involved in aminopeptidase A substrate specificity, *J Biol Chem*, 2009, **284**(16), 10618–10626.

37 Gao J, Marc Y, Iturrioz X, Leroux V, Balavoine F, *et al.*, A new strategy for treating hypertension by blocking the activity of the brain renin–angiotensin system with aminopeptidase A inhibitors, *Clin Sci*, 2014, **127**(3), 135–148.

38 Keck M, De Almeida H, Compère D, Inguimbert N, Flahault A, *et al.*, NI956/QGC006, a potent orally active, brain-penetrating aminopeptidase A inhibitor for treating hypertension, *Hypertension*, 2019, **73**, 1300-1307.

39 Velmourougane G, Harbut M B, Dalal S, McGowan S, Oellig C A, *et al.*, Synthesis of new (-)-Bestatin-based inhibitor libraries reveals a novel binding mode in the S1 pocket of the essential malaria M1 metalloamino peptidase, *J Med Chem*, 2011, **54**(6), 1655–1666.

40 Harbut M B, Velmourougane G, Dalal S, Reissa G, Whisstock J C, *et al.*, Bestatin-based chemical biology strategy reveals distinct roles for malaria M1- and M17-family aminopeptidases, *PNAS USA*, 2010, **108**(34), e526–e534.

41 Marchiò S, Lahdenranta J, Schlingemann R O, Valdembri D, Wesseling P, *et al.*, Aminopeptidase A is a functional target in angiogenic blood vessels, *Cancer Cell*, 2004, **5**(2), 151-162.

42 Takayasu S, Kazuhiko I, Kiyosumi S, Seiji N, Hiroaki K, *et al.*, Regulation of aminopeptidase A expression in cervical carcinoma: Role of tumor–stromal interaction and vascular endothelial growth factor, *Lab Invest*, 2004, **84**(5), 639–648.